

Cite this: *Org. Biomol. Chem.*, 2018, **16**, 9454

Meroterpene-like compounds derived from β -caryophyllene as potent α -glucosidase inhibitors†

Shuang-Jiang Ma,^{‡a} Jie Yu,^{‡a} Da-Wei Yan,^a Da-Cheng Wang,^a Jin-Ming Gao^{‡*a} and Qiang Zhang^{‡*a,b}

Meroterpenoids isolated from guava (*Psidium guajava*) and *Rhodomyrtus tomentosa* possess special skeletons which incorporate terpenoids with phloroglucinol derivatives. Most of these meroterpenoids showed high cytotoxicity against cancer cell lines. However, their chemical diversity is very limited. Herein, we employed a biomimetic hetero-cycloaddition starting from *ortho*-quinone methides and an abundant natural product, β -caryophyllene, to generate meroterpene-like compounds. Considering that the source plant has hyperglycemic functions, α -glucosidase was selected as a target for bioassay. Nine compounds were screened out for promising activities ($IC_{50} < 15 \mu M$), which were better than the positive controls genistein and acarbose. The best inhibitor **12** (IC_{50} 2.73 μM) possesses two caryophyllene moieties. They represented a new type of skeleton possessing activities against α -glucosidase. The kinetic study exhibited that these inhibitors belong to a non-competitive type. All these inhibitors may provide an opportunity to develop a new class of antidiabetic agents.

Received 30th October 2018,
Accepted 26th November 2018

DOI: 10.1039/c8ob02687d

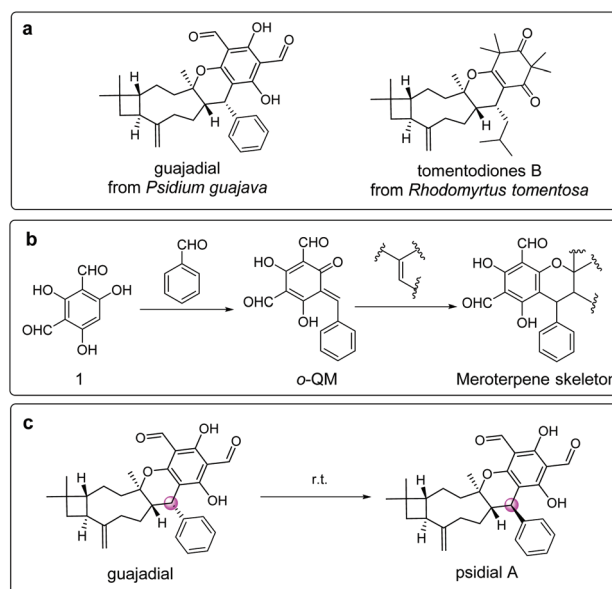
rsc.li/obc

Introduction

The chemical diversity of natural products (NPs) and their derivatives provides a huge contribution for developing novel drugs or lead compounds. However, the difficulty in obtaining novel scaffolds has recently declined in pharmaceutical research due to elaborate isolation procedures or lengthy pathways of total synthesis.^{1,2} Thus, it is urgently required to improve the diversity of NPs and their derivatives. In this regard, diversity-oriented synthesis (DOS) has emerged recently as an efficient strategy for constructing complex and diverse molecules from simple precursors.^{3,4} Easily accessible NPs as starting scaffolds are particularly effective for obtaining chemically diverse libraries that are useful in drug discovery.^{5–8} This strategy can avoid too many reaction steps for building complex scaffolds.^{6,9–12}

Meroterpenoids isolated from guava (*Psidium guajava*) and *Rhodomyrtus tomentosa* are a typical group of meroterpenoids

arising from phloroglucinols (Scheme 1a and b).^{13–23} Some of the meroterpene metabolites, such as the main meroterpene component (guajadial) from guava leaves (Fig. 1a), displayed



Scheme 1 Typical meroterpene skeletons from *Psidium guajava* and *Rhodomyrtus tomentosa*. (a) Representative meroterpenoid structures; (b) total synthesis pathway; (c) the epimerization of guajadial.

^aShaanxi Key Laboratory of Natural Products & Chemical Biology, College of Chemistry & Pharmacy, Northwest A&F University, Yangling 712100, PR China. E-mail: zhangq@mwsuaf.edu.cn, jinminggao@mwsuaf.edu.cn

^bState Key Laboratory of Medicinal Chemical Biology, Nankai University, Tianjin 300071, People's Republic of China

†Electronic supplementary information (ESI) available: ¹H and ¹³C NMR and HRMS spectra of products. CCDC 1838685–1838687. For ESI and crystallographic data in CIF or other electronic format see DOI: 10.1039/c8ob02687d

‡These authors contributed equally to this article.

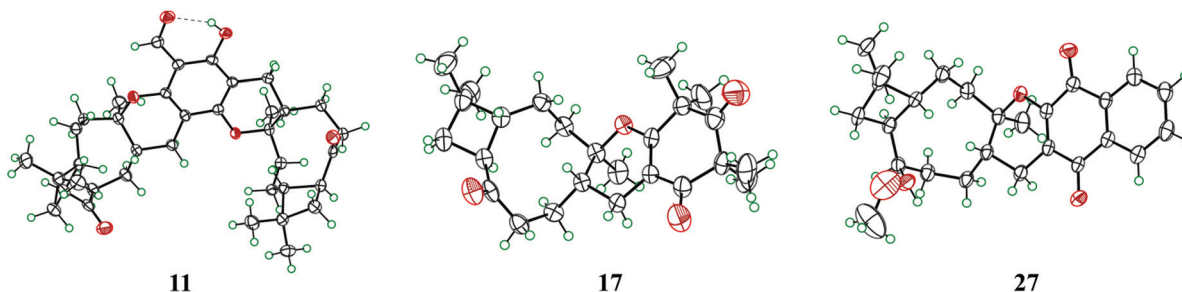


Fig. 1 X-ray ORTEP views of compounds 11, 17 and 27 (CCDC No. 1838685–1838687†).

high cytotoxicities against cancer cell lines *via* inhibiting the Top1 enzyme (IC_{50} 160 nM).¹⁴ Inspired by the hyperglycemic function of guava leaves in traditional Chinese medicine, we envisioned that the typical meroterpenes also have similar bioactivities. However, the compound guajadial is not so stable and tends to epimerize into another NP, psidial A (Scheme 1c).²⁴

In synthetic chemistry, these products were totally synthesized by a one-pot procedure from *ortho*-quinone methides (*o*-QM) and terpenoids (Scheme 1b).^{25,26} *o*-QMs are highly useful building blocks for the total synthesis of many natural products (NPs). Their inherent reactivity can be used in cascaded reactions for constructing complex scaffolds.²⁷ We selected three natural precursors of *o*-QM (*pre*-QM, Scheme 2a), which can also be regarded as privileged structures due to the high bioactivities of their derivatives. The *pre*-QMs 1 and 2 commonly exist in these natural meroterpenes. QM 3 is an essential moiety of the highly bioactive compound lapachol which showed potential against many targets, especially human cancer cells DU145 (IC_{50} 64 nM).²⁸ These *pre*-QMs can transform into *o*-QMs in the cascaded one-pot procedure to construct meroterpenes-like products. For the example of 3 (Scheme 2b), once compound 3 reacts with paraformaldehyde, the *o*-QM intermediate will generate immediately, which is followed by cycloaddition or Michael addition²⁵ on the vinyl of terpenoids to yield meroterpenes scaffolds.

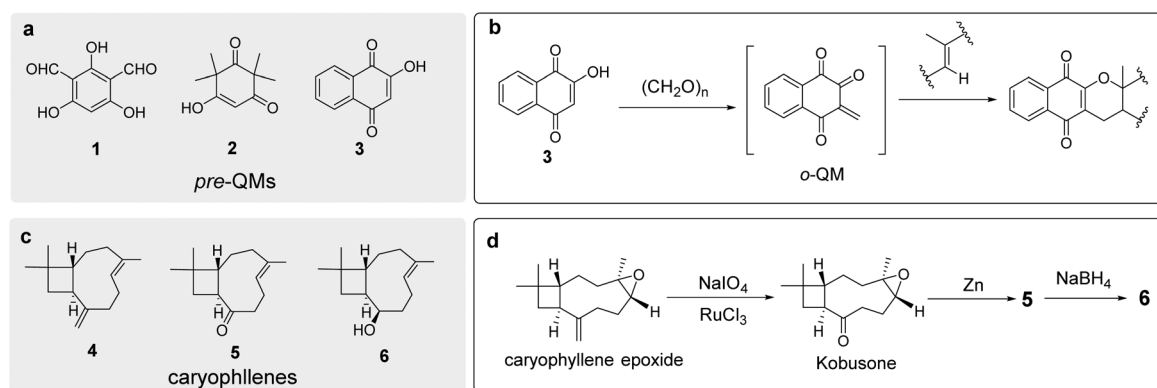
Besides the natural β -caryophyllene (4, Scheme 2c), two other derivatives (5 and 6) were synthesized (Scheme 2d) and employed as sesquiterpenoid building blocks to improve the diversity of the products.

Results and discussion

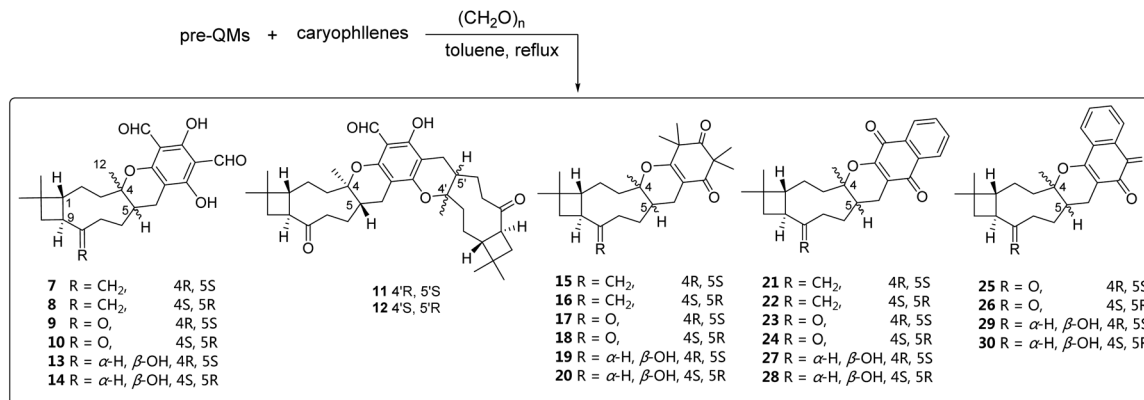
Synthesis of the meroterpenes-like compounds

The *pre*-QM building blocks 1 and 2 were synthesized according to the reported procedures.^{29–31} The derivatives of caryophyllene 5 and 6 were synthesized from caryophyllene epoxide whose terminal vinyl was cleared by $NaIO_4/RuCl_3$ and the epoxide group was reduced to vinyl by Zn powder (Scheme 2d). Due to the steric effect, the hydroxyl group in compound 6 is β -oriented (*R*), which was also indicated by the X-ray analysis of its derivative 27 (Fig. 1).

Every *pre*-QM was combined with every caryophyllene derivative respectively to afford 24 products, which can be classified into 5 different scaffolds (Scheme 3). Despite the total synthesis of these types of meroterpenes having been reported, obtaining enantioselective products is still difficult. On the other hand, the stereoisomers would enhance the diversity of products and help understand the relationship between the skeletons and the bioactivities. To recognize the absolute configurations (ACs) of these newly formed chiral



Scheme 2 (a) Selected *o*-QM precursors; (b) formation and reactivity of *o*-QM; (c) structures of β -caryophyllene (4) and its derivatives (5 and 6); (d) synthesis of the caryophyllene derivatives 5 and 6.



Scheme 3 Diversity-oriented synthesis of natural-like meroterpenes.

carbons (C-4 and C-5), we carried out NOESY, X-ray diffraction analysis, and ECD calculations.

Since the chiralities of C-1 and C-9 remained unchanged in the reactions (Scheme 3), they can be selected as inside reference groups for determining ACs. For all the compounds except for **11** and **12**, NOESY correlations can be recognized from H₃-12 or H-5 to H-1 or H-9, which indicate the ACs of the chiralities of C-4 and C-5. All these products possess chromophores close to the newly formed chiral carbons (C-4 and C-5); thus we also employed ECD spectra associated with quantum calculations to verify their ACs. As typical examples, we selected compounds **9**, **10**, **17**, **18**, **23** and **24** to analyze their theoretical CD spectra since these compounds possess the same sesquiterpenoid moiety. Due to different UV absorptions arising from the incorporated chromophores, these six compounds showed obvious Cotton effects at 307, 223, and 394 nm on the CD spectra, respectively (Fig. 2). The calculated theoretical spectra indicated that the (4*R*,5*S*)-products of pre-QMs **1** and **3** have negative CE at 307 nm and 394 nm respectively, while (4*S*,5*R*)-products have positive CE. However, the products synthesized from pre-QM **2** showed different negative CEs at 223 nm. It should be noted that these spectra showed almost mirror-image CD curves. In general, only those chirality

centers near chromophores, such as C-4 and C-5 in these compounds, can yield obvious CEs around their λ_{max}. The chiral centers at C-1 and C-9 are far away from the chromophores; thus they only give the CE at around 208 nm. Comprising these experimental ECD spectra with theoretical ECD curves, the consistency of the whole spectra (from 190 to 400 nm) allowed us to confirm their ACs as shown therein. Furthermore, X-ray diffraction of compound **17** also verified the whole configurations (Cu K_α, Flack coefficient 0.02).

When the pre-QM **1** was combined with the caryophyllene derivative **5**, more complex skeletons (**11** and **12**) were generated containing 2 caryophyllene substructures. The planar structure and configuration of compound **11** were verified by X-ray diffraction (Cu K_α, Flack coefficient 0.02, Fig. 1), which possesses (4*R*,5*S*,4'*R*,5'*S*)-stereochemistry. Product **12** showed much-closer ¹H NMR and ¹³C NMR spectra data to those of compound **11**, but they have different retention times (t_R) on an ordinary HPLC C₁₈ column, which indicated that the two compounds are diastereoisomers. The NOESY correlations shown in Fig. 3a indicated that H₃C-12, H-9, H-5' and H-9' are all on the same α-side of the caryophyllene macrocycle. In addition, the cycloaddition mechanism indicates that a *trans* double bond will yield *trans*-chiral centers (C-4/C-5 and C-4'/

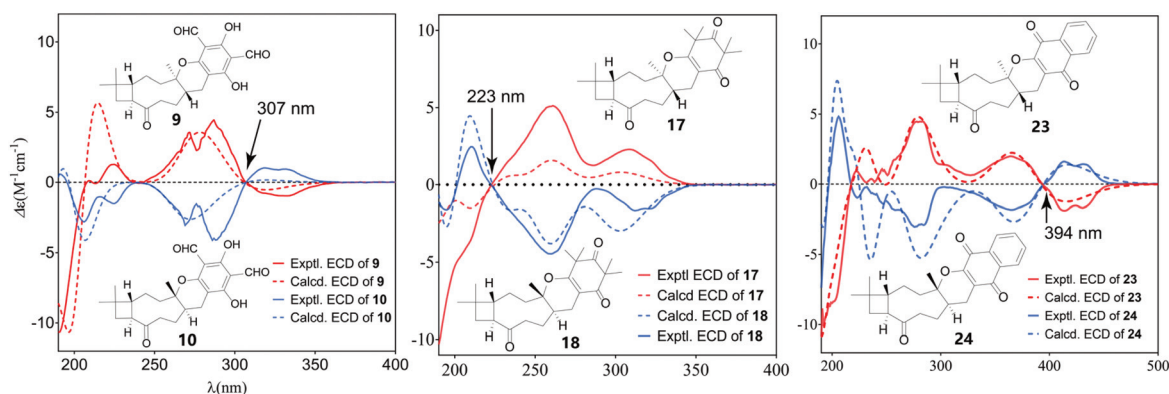


Fig. 2 Experimental and calculated ECD spectra of **9**, **10**, **17**, **18**, **23** and **24**. See Fig. S1 in the ESI† for the other ECD spectra.

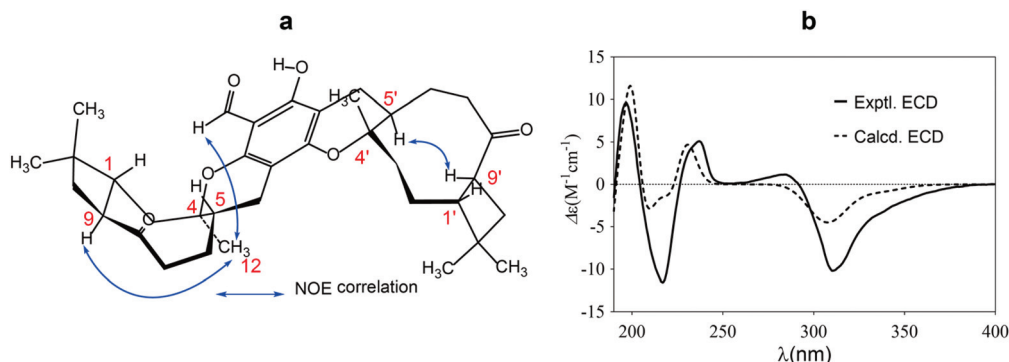


Fig. 3 (a) Selected NOESY correlations of **12**; (b) experimental and calculated ECD spectra of **12**.

C-5'). Thus, the configuration of **12** was determined as (4*R*,5*S*,4'*S*,5'*R*). Furthermore, the consistent CEs between the experimental and calculated spectra (Fig. 3b) confirmed the correct configuration assignment.

Evaluation of the α -glucosidase inhibiting effect of the natural-like compounds

α -Glucosidase is an important enzyme catalyzing carbohydrate digestion.³² Inhibiting this enzyme will postpone glucose absorption, and then lower postprandial blood glucose.^{33,34} α -Glucosidase inhibitors such as acarbose, miglitol, and voglibose are being utilized as oral antidiabetic drugs. To screen out lead compounds from the synthetic products, all the compounds were primarily bioassayed on this enzyme at 25 and

50 μ M concentrations. The compounds listed in the table showed a high inhibition rate (more than 50%) at 25 μ M level; thus, they were evaluated further for IC_{50} values. Except compound **22**, they all showed higher inhibition than the positive control genistein and the drug acarbose (Table 1). In particular, the polycyclic compounds **11**, **12** and **29** showed potent activity against α -glucosidase with IC_{50} values ranging from 2.7 to 5.4 μ M.

In the primary screening, the building blocks 1–6 have not been found to have any inhibition on the α -glucosidase enzyme. Only when these *pre*-QMs (**1–3**) were combined with terpenoid moieties 4–6 to form meroterpenoid-like products, obvious inhibition was detected. These indicated that both the *pre*-QMs and terpenoid moieties are essential for bioactivity. Although the *pre*-QM moiety in the meroterpenoid skeletons provides binding sites for hydrogen bonds, the terpenoid moieties are also essential due to their hydrophobic interaction with the target enzyme. In particular, compounds **11** and **12** possess more large hydrophobic substructures, which contribute to their high activities. The chiralities of C-4 and C-5 may have limited influence on the bioactivities, such as pairs of compounds **11/12** and **25/26**, which showed similar bioactivities.

To explore the interaction mechanism of the typical products **12** and **21** with high activities, the enzyme kinetic studies were carried out using the Lineweaver–Burk plot ana-

Table 1 IC_{50} against α -glucosidase

	IC_{50} (μ M)		IC_{50} (μ M)
11	5.42 ± 0.71	26	6.57 ± 0.66
12	2.73 ± 0.13	28	9.24 ± 0.50
13	9.47 ± 0.64	29	3.32 ± 0.25
21	8.82 ± 0.48	G	22.64 ± 3.03
22	13.95 ± 1.47	A	>50
25	11.92 ± 0.30		

G, genistein, A, acarbose.

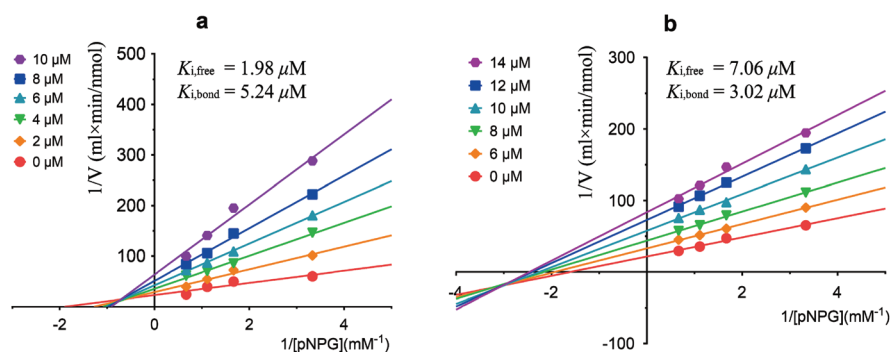


Fig. 4 Lineweaver–Burk plot analysis of the kinetics of α -glucosidase inhibition exerted by compounds **12** (a) and **21** (b).

lysis.^{35,36} α -Glucosidase was treated with pNPG at various concentrations (0.3–1.5 mM) in the absence or presence of **12** and **21** at five different concentrations. As shown in Fig. 4, **12** and **21** showed a noncompetitive type of inhibition against α -glucosidase. Replotting the slope and *Y*-intercept values taken from each line in the primary Lineweaver–Burk plot (see the ESI†) allowed extrapolation of the inhibition constants $K_{i,free}$ (a measure of the affinity to the free enzyme) and $K_{i,bound}$ (a measure of the affinity to the complex enzyme–substrate). The $K_{i,free}$ and $K_{i,bound}$ values of **12** were 1.98 and 5.24 μ M, whereas the values of compound **21** were 7.06 and 3.02 μ M.

Conclusions

In conclusion, we have reported the construction of a set of meroterpenoid-like compounds starting from caryophyllene and natural essential moieties. All 24 products represent the creation of five different frameworks prepared in a biomimetic reaction, thereby providing the candidates to identify potentially new chemotypes. Due to the limited stereoselectivity of the construction reaction, all the ACs of the products were determined unambiguously by ECD calculations or X-ray diffraction analysis. Furthermore, the commercial availability of the starting materials allowed us to scale up reactions and obtain sufficient amounts of compounds for further investigations. Eight of the products, **11**, **12**, **13**, **21**, **25**, **26**, **28** and **29**, showed potential activities against α -glucosidase, which could be considered as promising lead compounds for developing new antidiabetic drugs. Furthermore, our findings have demonstrated that combining the abundant terpenoids with natural essential substructures will conveniently expand the chemical space of NPs and generate diverse skeletons covering potential lead compounds for further development.

Experimental

General procedure

NMR spectra were recorded in $CDCl_3$ using an AVANCE III spectrometer (400 MHz) and an AVANCE III spectrometer (500 MHz). TMS was used as an internal reference for chemical shifts (in ppm). Coupling constants, *J*, are reported in hertz (Hz). Melting points were determined using a MEL-TEMP 1101D apparatus and are uncorrected. ESI-MS spectra were recorded on a Thermo Fisher Scientific LTQ Fleet instrument. HR ESIMS data were obtained by using an AB Sciex Triple TOF 4600 system. Optical rotations were measured on a PerkinElmer 341 polarimeter with a thermally jacketed 5 cm cell at approximately 20 °C, and concentrations (*c*) are given in g per 100 ml. ECD spectra were obtained on a Chirascan CD spectrometer. Crystallographic data were collected on a Bruker Smart Apex CCD area detector diffractometer with graphite-monochromated Cu K α radiation ($\lambda = 1.54184$ Å) at 293(2) K using the ω -scan technique. Crystal structures were solved and refined by SHELXT and SHELXS³⁷ associated with Olex² as a

GUI tool. Column chromatography was performed on silica gel (90–150 μ m) and Chromatorex C₁₈ gel (40–75 μ m). GF₂₅₄ plates were used for thin-layer chromatography (TLC). HPLC analysis and preparations were performed on a Waters 1525 instrument.

Preparation of meroterpenoid-like products 7–30

To a solution of 1.1 mmol pre-QM in 1,4-dioxane (3.0 ml) was added paraformaldehyde (774 mg) and 3 eq. β -caryophyllene (or its derivative). After being stirred under reflux for 24 h, the solvent was removed from the reaction mixture under vacuum. The crude products were separated on a silica gel column (PE–EtOAc from 50 : 1 to 10 : 1) and a semi-HPLC C₁₈ column (gradient MeCN 80–100%) repeatedly to yield pure products. The spectra data of compounds **9**, **11**, **17** and **25** were selected as representative examples listed as below. For the full list of all the synthetic products, please find them in the ESI.†

Compound 9. Colorless oil (53 mg, 12%); $[\alpha]_D^{20} = -47.0$ (*c* 0.05 in CH_3CN); UV $\lambda_{max}(MeCN)/nm$ ($\log \epsilon$) 277 (4.51), 344 (3.43); ¹H NMR (400 MHz, $CDCl_3$) δ ppm 1.00 (s, 3 H), 1.02 (s, 3 H), 1.24 (s, 3 H), 1.45 (dd, *J* = 10.96, 7.43 Hz, 1 H), 1.55–1.66 (m, 1 H), 1.73–1.95 (m, 4 H), 2.01–2.24 (m, 4 H), 2.25–2.34 (m, 1 H), 2.46 (dt, *J* = 13.69, 5.67 Hz, 1 H), 2.72 (dd, *J* = 16.63, 4.89 Hz, 1 H), 2.77–2.86 (m, 1 H), 3.08–3.18 (m, 1 H), 10.00 (s, 1 H), 10.14 (s, 1 H), 13.23 (s, 1 H), 13.39 (s, 1 H); ¹³C NMR (100 MHz, $CDCl_3$) δ ppm 21.2, 21.9, 22.7, 23.6, 29.6, 29.6, 31.6, 34.6, 35.0, 37.3, 41.3, 46.0, 50.7, 83.9, 100.2, 103.7, 103.9, 162.6, 168.1, 168.4, 191.6, 191.6, 212.7; HRESIMS *m/z* [*M* + *H*]⁺ calcd for C₂₃H₂₉O₆ 401.1964, found 401.1968.

Compound 11. Colorless oil (78 mg, 12%); $[\alpha]_D^{20} = -78.0$ (*c* 0.05 in CH_3CN); UV $\lambda_{max}(MeCN)/nm$ ($\log \epsilon$) 304(4.31); ¹H NMR (400 MHz, $CDCl_3$) δ ppm 0.99 (s, 3 H), 1.01 (s, 3 H), 1.05 (s, 6 H), 1.15 (s, 6 H), 1.44 (dt, *J* = 11.0, 8.2 Hz, 2 H), 1.50–1.63 (m, 2 H), 1.63–1.75 (m, 2 H), 1.76–1.93 (m, 5 H), 1.93–2.00 (m, 1 H), 2.00–2.10 (m, 3 H), 2.10–2.17 (m, 2 H), 2.17–2.30 (m, 4 H), 2.38–2.49 (m, 2 H), 2.53 (dd, *J* = 16.6, 5.3 Hz, 1 H), 2.72–2.80 (m, 2 H), 2.83–2.92 (m, 1 H), 3.04–3.20 (m, 2 H), 12.46 (s, 1 H); ¹³C NMR (100 MHz, $CDCl_3$) δ ppm 20.8, 21.3, 21.7, 22.1, 22.7, 22.8, 24.0, 25.2, 29.7, 29.7, 29.8, 30.2, 31.5, 31.8, 34.5, 34.7, 35.2, 35.4, 37.4, 37.4, 41.3, 41.3, 45.4, 46.7, 50.7, 50.7, 80.6, 81.9, 100.0, 100.0, 100.1, 154.7, 159.0, 160.6, 191.4, 213.1, 213.4; HR ESI-MS *m/z* [*M* + *H*]⁺ calcd for C₃₇H₅₁O₆ 591.3686, found 591.3689.

Compounds 17. White solid (229 mg, 52%), $[\alpha]_D^{20} = +27.4$ (*c* 0.05 in CH_3CN); UV $\lambda_{max}(MeCN)/nm$ ($\log \epsilon$) 261(4.12); ¹H NMR (400 MHz, $CDCl_3$) δ ppm 0.99 (s, 3 H), 1.01 (s, 3 H), 1.14 (s, 3 H), 1.31 (s, 3 H), 1.32 (s, 3 H), 1.34 (s, 3 H), 1.36 (s, 3 H), 1.44 (dd, *J* = 11.0, 7.4 Hz, 1 H), 1.51–1.62 (m, 1 H), 1.62–1.70 (m, 1 H), 1.74 (dtd, *J* = 11.7, 5.9, 5.9, 3.1 Hz, 2 H), 1.78–1.89 (m, 2 H), 2.00–2.08 (m, 1 H), 2.09–2.16 (m, 1 H), 2.17–2.28 (m, 2 H), 2.43 (dt, *J* = 13.7, 5.9 Hz, 1 H), 2.54 (dd, *J* = 17.0, 5.3 Hz, 1 H), 2.72–2.83 (m, 1 H), 3.08–3.19 (m, 1 H); ¹³C NMR (100 MHz, $CDCl_3$) δ ppm 20.7, 21.9, 22.5, 23.8, 24.6, 25.2, 25.3, 25.4, 29.1, 29.4, 31.8, 34.6, 35.5, 36.9, 41.4, 46.1, 47.4, 50.7, 54.8, 83.0, 106.7, 169.8, 197.4, 212.9, 213.5; HR ESI-MS *m/z* [*M* + *H*]⁺ calcd for C₂₅H₃₇O₄ 401.2692, found 401.2696.

Compound 25. Rufous solid (21 mg, 5%), $[\alpha]_D^{20} = -44.6$ (c 0.05 in CH_3CN); UV $\lambda_{\text{max}}(\text{MeCN})/\text{nm}$ ($\log \epsilon$) 257(4.30); ^1H NMR (500 MHz, CDCl_3) δ ppm 0.99 (s, 3 H), 1.04 (s, 3 H), 1.28 (s, 3 H), 1.46 (dd, $J = 11.0, 7.6$ Hz, 1 H), 1.62–1.71 (m, 1 H), 1.75–1.97 (m, 4 H), 2.06 (dd, $J = 17.3, 11.0$ Hz, 1 H), 2.15 (t, $J = 10.2$ Hz, 1 H), 2.19–2.27 (m, 2 H), 2.31–2.40 (m, 1 H), 2.43–2.51 (m, 1 H), 2.71–2.85 (m, 2 H), 3.12–3.20 (m, 1 H), 7.52 (t, $J = 7.6$ Hz, 1 H), 7.65 (td, $J = 7.7, 1.3$ Hz, 1 H), 7.76 (d, $J = 7.9$ Hz, 1 H), 8.04–8.09 (m, 1 H); ^{13}C NMR (125 MHz, CDCl_3) δ ppm 21.3, 21.8, 22.7, 24.6, 29.4, 29.6, 31.7, 34.7, 35.3, 37.3, 41.2, 45.8, 50.7, 84.9, 112.6, 123.8, 128.7, 130.2, 130.8, 132.2, 134.8, 161.4, 178.0, 179.7, 212.6; HR ESI-MS m/z $[\text{M} + \text{H}]^+$ calcd for $\text{C}_{25}\text{H}_{29}\text{O}_4$ 393.2066, found 393.2065.

ECD calculation method

All the conformers of every calculated compound were searched by Conflex using the MMFF94s force field.^{38,39} Further optimization were performed at the B3LYP/6-31+G(d,p) level in Gaussian 09 package.⁴⁰ The theoretical CD spectra were calculated by cam-B3LYP/TZVP and summated in SpecDis⁴¹ according to their Boltzmann-calculated distributions.

α -Glucosidase inhibitory assay

The α -glucosidase inhibitory assay of the synthesized compounds was performed as reported in the literature.³⁶ Briefly, α -glucosidase was purchased from Sigma (EC 3.2.1.20), which was isolated from *Saccharomyces cerevisiae*. The enzyme was dissolved in 200 μL of 10 mM phosphate buffer (pH 6.80) and incubated in the presence of 12 μL of the test compound in DMSO at 37 $^\circ\text{C}$ for 5 min. The reaction was started by the addition of 36 μL of 4-nitrophenyl α -D-glucopyranoside (p-NPG) and maintained under 37 $^\circ\text{C}$ for 40 min. The amount of released 4-nitrophenol was measured as the absorbance at 400 nm. The assay was performed with 5 or 6 different concentrations around the IC_{50} values, approximately estimated in previous experiments. In each set of experiments, the assay was performed in triplicate and at least three times. The increased absorbance was compared with that of the control containing 12 μL of DMSO in the place of the test solution. The percentage inhibition of α -glucosidase activity was calculated *via* the following formula: Inhibition ratio (%) = $100 \times (A_{\text{control}} - A_{\text{sample}})/A_{\text{control}}$. The IC_{50} values were calculated in Prism 7 using a nonlinear regression method with the normalized response and variable slope.

Kinetic analysis of α -glucosidase inhibition

The kinetic parameters of α -glucosidase inhibition by compounds **12** and **21** were evaluated by the Lineweaver–Burk plots and its secondary plots. The double-reciprocal plots were constructed with enzyme reaction initial velocity (V) *versus* substrate (S) concentration ($1/\nu$ vs. $1/[S]$) in the absence (control) or in the presence of **12** and **21** at different concentrations (5–10 μM). The initial rate was measured by stopping the reaction after 2 min. The type of inhibition and K_m and V_{max} values were determined from the plots. The slopes and

Y -intercepts of these reciprocal plots were also replotted against the inhibitor concentration, respectively. Data analysis was performed using Prism software.

Conflicts of interest

There are no conflicts to declare.

Acknowledgements

This work is financially supported by the Natural Science and Basic Research Plan of Shaanxi Province (No. 2016JM2002) and the State Key Laboratory of Medicinal Chemical Biology (Nankai University, No. 201502003).

Notes and references

- C. R. Pye, M. J. Bertin, R. S. Lokey, W. H. Gerwick and R. G. Linington, *Proc. Natl. Acad. Sci. U. S. A.*, 2017, **114**, 5601.
- J. W.-H. Li and J. C. Vederas, *Science*, 2009, **325**, 161.
- J. Kim, H. Kim and S. B. Park, *J. Am. Chem. Soc.*, 2014, **136**, 14629.
- W. R. J. D. Galloway, A. Isidro-Llobet and D. R. Spring, *Nat. Commun.*, 2010, **1**, 80.
- X. Zhang and S. Li, *Nat. Prod. Rep.*, 2017, **34**, 1061.
- H. Kikuchi, T. Nishimura, E. Kwon, J. Kawai and Y. Oshima, *Chem. – Eur. J.*, 2016, **22**, 15819.
- G. Prabhu, S. Agarwal, V. Sharma, S. M. Madurkar, P. Munshi, S. Singh and S. Sen, *Eur. J. Med. Chem.*, 2015, **95**, 41.
- K. C. Morrison and P. J. Hergenrother, *Nat. Prod. Rep.*, 2014, **31**, 6.
- Q. Zhang, H.-Y. Tang, M. Chen, J. Yu, H. Li and J.-M. Gao, *Org. Biomol. Chem.*, 2017, **15**, 4456.
- S.-J. Ma, J. Yu, H.-F. Fan, Z.-H. Li, A.-L. Zhang and Q. Zhang, *RSC Adv.*, 2017, **7**, 40510.
- H.-Y. Tang, J.-M. Gao and Q. Zhang, *RSC Adv.*, 2015, **5**, 72433.
- H.-Y. Tang, L.-L. Quan, J. Yu, Q. Zhang and J.-M. Gao, *J. Mol. Struct.*, 2018, **1155**, 675.
- G.-H. Tang, Z. Dong, Y.-Q. Guo, Z.-B. Cheng, C.-J. Zhou and S. Yin, *Sci. Rep.*, 2017, **7**, 1047.
- X.-J. Qin, Q. Yu, H. Yan, A. Khan, M.-Y. Feng, P.-P. Li, X.-J. Hao, L.-K. An and H.-Y. Liu, *J. Agric. Food Chem.*, 2017, **65**, 4993.
- Y.-Q. Jian, X.-J. Huang, D.-M. Zhang, R.-W. Jiang, M.-F. Chen, B.-X. Zhao, Y. Wang and W.-C. Ye, *Chem. – Eur. J.*, 2015, **21**, 9022.
- Y. Gao, G.-T. Li, Y. Li, P. Hai, F. Wang and J.-K. Liu, *Nat. Prod. Bioprospect.*, 2013, **3**, 14.
- M. Shao, Y. Wang, Y.-Q. Jian, X.-J. Huang, D.-M. Zhang, Q.-F. Tang, R.-W. Jiang, X.-G. Sun, Z.-P. Lv, X.-Q. Zhang and W.-C. Ye, *Org. Lett.*, 2012, **14**, 5262.

- 18 Y. Gao, G.-Q. Wang, K. Wei, P. Hai, F. Wang and J.-K. Liu, *Org. Lett.*, 2012, **14**, 5936.
- 19 M. Shao, Y. Wang, Z. Liu, D.-M. Zhang, H.-H. Cao, R.-W. Jiang, C.-L. Fan, X.-Q. Zhang, H.-R. Chen, X.-S. Yao and W.-C. Ye, *Org. Lett.*, 2010, **12**, 5040.
- 20 H.-Z. Fu, Y.-M. Luo, C.-J. Li, J.-Z. Yang and D.-M. Zhang, *Org. Lett.*, 2010, **12**, 656.
- 21 X.-L. Yang, K.-L. Hsieh and J.-K. Liu, *Org. Lett.*, 2007, **9**, 5135.
- 22 Y.-L. Zhang, C. Chen, X.-B. Wang, L. Wu, M.-H. Yang, J. Luo, C. Zhang, H.-B. Sun, J.-G. Luo and L.-Y. Kong, *Org. Lett.*, 2016, **18**, 4068.
- 23 H.-X. Liu, K. Chen, G.-H. Tang, Y.-F. Yuan, H.-B. Tan and S.-X. Qiu, *RSC Adv.*, 2016, **6**, 48231.
- 24 A. L. Lawrence, R. M. Adlington, J. E. Baldwin, V. Lee, J. A. Kershaw and A. L. Thompson, *Org. Lett.*, 2010, **12**, 1676.
- 25 C. G. Newton, D. N. Tran, M. D. Wodrich and N. Cramer, *Angew. Chem., Int. Ed.*, 2017, **56**, 13776.
- 26 H. C. Lam, J. T. J. Spence and J. H. George, *Angew. Chem., Int. Ed.*, 2016, **55**, 10368.
- 27 N. J. Willis and C. D. Bray, *Chem. – Eur. J.*, 2012, **18**, 9160.
- 28 K. O. Eyong, P. S. Kumar, V. Kuete, G. N. Folefoc, E. A. Nkengfack and S. Baskaran, *Bioorg. Med. Chem. Lett.*, 2008, **18**, 5387.
- 29 C. Dittmer, G. Raabe and L. Hintermann, *Eur. J. Org. Chem.*, 2007, 5886.
- 30 H. Müller, M. Paul, D. Hartmann, V. Huch, D. Blaesius, A. Koeberle, O. Werz and J. Jauch, *Angew. Chem., Int. Ed.*, 2010, **49**, 2045.
- 31 N. Duhamel, D. Martin, R. Larcher, B. Fedrizzi and D. Barker, *Tetrahedron Lett.*, 2016, **57**, 4496.
- 32 J. Wei, X.-Y. Zhang, S. Deng, L. Cao, Q.-H. Xue and J.-M. Gao, *Nat. Prod. Res.*, 2017, **31**, 2062.
- 33 D. Halegoua-De Marzio and V. J. Navarro, in *Drug-Induced Liver Disease*, ed. N. Kaplowitz and L. D. DeLeve, Academic Press, Boston, 3rd edn, 2013, pp. 519–540.
- 34 J.-L. Chiasson, *Ann. Intern. Med.*, 1994, **121**, 928.
- 35 X.-Q. Zhang, X.-F. Mou, N. Mao, J.-J. Hao, M. Liu, J.-Y. Zheng, C.-Y. Wang, Y.-C. Gu and C.-L. Shao, *Eur. J. Med. Chem.*, 2018, **146**, 232.
- 36 C. Tavani, L. Bianchi, A. De Palma, G. I. Passeri, G. Punzi, C. L. Pierri, A. Lovece, M. M. Cavalluzzi, C. Franchini, G. Lentini and G. Petrillo, *Bioorg. Med. Chem. Lett.*, 2017, **27**, 3980.
- 37 G. M. Sheldrick, *Acta Crystallogr., Sect. C: Struct. Chem.*, 2015, **71**, 3.
- 38 CONFLEX, Conflex corp., Tokyo-Yokohama, JAPAN.
- 39 H. Gotō and E. Ōsawa, *J. Chem. Soc., Perkin Trans. 2*, 1993, 187.
- 40 *Gaussian 09, Revision D.01*, Gaussian, Inc., Wallingford CT, 2013, see the ESI for full citation.†
- 41 T. Bruhn, A. Schaumlöffel, Y. Hemberger and G. Bringmann, *Chirality*, 2013, **25**, 243.